



THE UNIVERSITY *of* EDINBURGH

## Edinburgh Research Explorer

### Polymorphism in the crystal structures of the group 13 trimethyls

**Citation for published version:**

Boese, R, Downs, AJ, Greene, TM, Hall, AW, Morrison, CA & Parsons, S 2003, 'Polymorphism in the crystal structures of the group 13 trimethyls', *Organometallics*, vol. 22, no. 12, pp. 2450-2457.  
<https://doi.org/10.1021/om0300272>

**Digital Object Identifier (DOI):**

[10.1021/om0300272](https://doi.org/10.1021/om0300272)

**Link:**

[Link to publication record in Edinburgh Research Explorer](#)

**Document Version:**

Peer reviewed version

**Published In:**

Organometallics

**Publisher Rights Statement:**

Copyright © 2003 by the American Chemical Society. All rights reserved.

**General rights**

Copyright for the publications made accessible via the Edinburgh Research Explorer is retained by the author(s) and / or other copyright owners and it is a condition of accessing these publications that users recognise and abide by the legal requirements associated with these rights.

**Take down policy**

The University of Edinburgh has made every reasonable effort to ensure that Edinburgh Research Explorer content complies with UK legislation. If you believe that the public display of this file breaches copyright please contact [openaccess@ed.ac.uk](mailto:openaccess@ed.ac.uk) providing details, and we will remove access to the work immediately and investigate your claim.



This document is the Accepted Manuscript version of a Published Work that appeared in final form in *Organometallics*, copyright © American Chemical Society after peer review and technical editing by the publisher. To access the final edited and published work see <http://dx.doi.org/10.1021/om0300272>

Cite as:

Boese, R., Downs, A. J., Greene, T. M., Hall, A. W., Morrison, C. A., & Parsons, S. (2003). Polymorphism in the crystal structures of the group 13 trimethyls. *Organometallics*, 22(12), 2450-2457.

Manuscript received: 14/01/2003; Article published: 09/06/2003

## Polymorphism in the Crystal Structures of the Group 13 Trimethyls\*\*

Roland Boese,<sup>1</sup> Anthony J. Downs,<sup>2</sup> Timothy M. Greene,<sup>3</sup> Carole A. Morrison<sup>4</sup> and Simon Parsons<sup>4</sup>

<sup>[1]</sup>Institut für Anorganische Chemie, Universität Essen, Universitätsstrasse 3-5, 45117 Essen, Germany

<sup>[2]</sup>Inorganic Chemistry Laboratory, University of Oxford, South Parks Road, Oxford, England OX1 3QR, UK.

<sup>[3]</sup>School of Chemistry, University of Exeter, Chemistry Building, Stocker Road, Exeter, England EX4 4QD, UK.

<sup>[4]</sup>EaStCHEM, School of Chemistry, Joseph Black Building, University of Edinburgh, West Mains Road, Edinburgh, EH9 3JJ, UK.

<sup>[\*]</sup>Corresponding author; e-mail: [s.parsons@ed.ac.uk](mailto:s.parsons@ed.ac.uk), tel: 0131 650 5804, fax: 0131 650 4806

<sup>[\*\*]</sup>We thank the EPSRC for research funding and for an Advanced Fellowship to T.M.G. and the Royal Society for a University Research Fellowship to C.A.M.

### Supporting information:

Tables giving crystallographic data for BMe<sub>3</sub>, GaMe<sub>3</sub>, and TlMe<sub>3</sub> and optimized theoretical coordinates for polymorphs of BMe<sub>3</sub>, GaMe<sub>3</sub>, and InMe<sub>3</sub>. This material is available free of charge via the Internet at <http://pubs.acs.org>

## Abstract

Crystal structures have been determined for trimethylboron,  $\text{BMe}_3$ , and for a new polymorph of trimethylgallium,  $\text{GaMe}_3$ ; in addition, the crystal structure of trimethylthallium,  $\text{TlMe}_3$ , has been redetermined. The  $\text{BMe}_3$  crystal structure represents a new structural type for the group 13 trimethyl derivatives in the solid state. In contrast to its heavier analogues, it consists of layers containing only very weakly interacting  $\text{BMe}_3$  molecules.  $\text{GaMe}_3$  forms a ladder-like pseudo-polymer via long gallium-to-methyl intermolecular interactions with  $\text{Ga}\cdots\text{C}$  distances in the range 3.096(3)–3.226(4) Å. This is compared with a recently reported crystal structure of a polymorph, which, like  $\text{InMe}_3$  and  $\text{TlMe}_3$ , is characterized by the formation of pseudo-tetramers. The effects of crystallization and secondary interactions have been analyzed by comparison with related crystallographic, gas-phase electron diffraction, and spectroscopic studies of these and other trimethyl derivatives of the group 13 elements. The energetic differences between polymorphs of  $\text{BMe}_3$ ,  $\text{GaMe}_3$ , and  $\text{InMe}_3$  have been explored by plane wave DFT calculations. The energy differences between the  $\text{BMe}_3$ -like layered structure and the  $\text{InMe}_3$ -like pseudo-tetrameric structure are calculated to be  $-1.7$ ,  $+3.6$ , and  $+10.4$  kJ mol $^{-1}$  for  $\text{BMe}_3$ ,  $\text{GaMe}_3$ , and  $\text{InMe}_3$ , respectively.

## Introduction

There are three different structures that are observed for the group 13 trimethyl derivatives in the crystalline state. One is the dimeric form observed for trimethylaluminum,<sup>1</sup> in which methyl groups participate in strong metal–metal bridges, with C–Al interaction distances commensurate with those of terminal Al–C bonds. Methyl bridging is also observed in a second structural type featured by the derivatives with Ga, In, and Tl, but the interaction distances are substantially longer than the primary metal–carbon bonds. Prior to this study, crystal structures had been determined for  $\text{GaMe}_3$ ,<sup>2</sup>  $\text{InMe}_3$ ,<sup>3,4</sup> and  $\text{TlMe}_3$ ,<sup>5</sup> here we describe crystal structure determinations of a new polymorph of  $\text{GaMe}_3$  and a redetermination of the structure of  $\text{TlMe}_3$ . The third structural type is represented by  $\text{BMe}_3$ . As we show below, this crystal structure consists of layers in which the molecules interact by weak van der Waals, or possibly electrostatic, interactions. The longstanding debate over the nature and geometry of the bridging methyl groups in  $\text{Al}_2\text{Me}_6$  has recently been resolved in a neutron powder diffraction study at 4.5 K,<sup>6</sup> and in this paper we limit our attention to the second and third structural types.

We have also investigated theoretically the energetic differences between polymorphs of  $\text{BMe}_3$ ,  $\text{GaMe}_3$ , and  $\text{InMe}_3$  in which the molecules form layers (as in the observed structure of  $\text{BMe}_3$ ) or weak methyl bridges (as in  $\text{InMe}_3$ ). Polymorphism has been described as the supramolecular equivalent of molecular isomerism.<sup>7</sup> Traditional ab initio modeling procedures (notably GAUSSIAN) simulate isolated molecules, but while this style of calculation is suitable for studying gaseous isomers, it is not so readily applicable to solids. Plane wave density functional theory (DFT) can simulate the periodic wave function characteristics of a repeating

unit such as a crystallographic unit cell. The lattice parameters and atomic positions can all be varied to minimize the crystal lattice energy, atomic forces, and unit cell stress, and we therefore use these methods to draw energetic comparisons between trimethyl polymorphs.

Our results complete the series of crystal structures for the group 13 trimethyls. The trimesityls (mesityl = 2,4,6-trimethylphenyl) are the only other group 13 organometallics for which a complete series of crystal structures has been determined.

## Experimental Section

### *Synthesis of Compounds*

(i) **Trimethylboron** was prepared by direct metathesis between trimethylaluminum (obtained from Aldrich and purified by fractional condensation in vacuo) and tri-*n*-butyl borate (also obtained from Aldrich) as neat liquids.<sup>8</sup> To moderate the exothermic reaction, the mixture was held in a Pyrex glass vessel fitted with a greaseless (Young's) valve at temperatures <233 K. Trimethylboron was the only volatile product. It was purified by fractional condensation in vacuo with traps held at 162, 144, and 77 K. The fraction collected at 144 K was identified as essentially pure trimethylboron on the evidence of the IR spectrum of the vapor.<sup>9</sup>

(ii) **Trimethylgallium** was prepared similarly by ligand redistribution between trimethylaluminum and gallium(III) chloride (obtained from Aldrich).<sup>10</sup> Warming the mixture to room temperature caused a vigorous reaction to occur. After the mixture was stirred for 90 min to ensure completion of the reaction, the volatile products were vaporized in vacuo and fractionated via traps held at 222, 178, and 77 K. Trimethylgallium was collected at 178 K and was authenticated by the IR spectrum of the vapor.<sup>11</sup>

(iii) **Trimethylthallium** was synthesized rather differently, namely in accordance with eq 1 by the addition of an excess of methyllithium in ether solution (1.4 M) to thallium(I) iodide in the presence of iodomethane (all reagents being used as supplied by Aldrich).<sup>12</sup>
$$2\text{MeLi} + \text{TlI} + \text{MeI} \rightarrow \text{TlMe}_3 + 2\text{LiI} \quad (1)$$
After the mixture had been stirred for 1 h at room temperature, the ether solution was siphoned off into a clean, preconditioned Schlenk tube. The solvent was evaporated under reduced pressure and the trimethylthallium isolated as a crystalline solid by fractionation in vacuo, being retained by a trap held at 242 K. The purity of the product was checked by reference to the IR spectrum of its vapor at ambient temperatures.<sup>13</sup>

### *Crystal Growth*

Samples of BMe<sub>3</sub>, GaMe<sub>3</sub>, and TlMe<sub>3</sub> were loaded into Pyrex capillaries and mounted on a Bruker Smart Apex CCD diffractometer equipped with an Oxford Cryosystems low-temperature device.<sup>14</sup> The boron and

gallium compounds (the former being a gas and the latter a liquid under ambient conditions) were respectively frozen at 100 and 213 K, and crystals were grown in situ by means of Boese's zone refinement method using an OHCD infrared laser-assisted crystallization device.<sup>15</sup> The sample of TlMe<sub>3</sub> was treated similarly, but since this tended to sublime rather than melt under laser irradiation, a suitable crystal was obtained by careful sublimation inside the capillary at 273 K. Data collections were carried out using graphite-monochromated Mo K $\alpha$  radiation ( $\lambda = 0.71073$  Å); collection parameters are listed in Table 1 or in the Supporting Information.

**Table 1.** Crystallographic Data Collection and Refinement Parameters

	BMe <sub>3</sub>	GaMe <sub>3</sub>	TlMe <sub>3</sub>
formula	C <sub>3</sub> H <sub>9</sub> B	C <sub>3</sub> H <sub>9</sub> Ga	C <sub>3</sub> H <sub>9</sub> Tl
$M_r$	55.91	114.82	249.47
cryst syst	monoclinic	monoclinic	tetragonal
space group	$C2/c$	$C2/c$	$P4_2/n$
$a/\text{\AA}$	6.3473(9)	18.409(3)	13.3049(7)
$b/\text{\AA}$	10.9284(16)	6.2652(9)	13.3049(7)
$c/\text{\AA}$	14.224(2)	18.268(3)	6.2891(5)
$\beta/\text{deg}$	91.099(3)	91.361(2)	90
$V/\text{\AA}^3$	986.5(2)	2106.4(5)	1113.30(12)
$T/\text{K}$	95	120	150
$Z$	8	16	8
$D_c/\text{Mg m}^{-3}$	0.753	1.448	2.977
$\mu/\text{mm}^{-1}$	0.038	5.044	28.844
range of transmissn	0.396–1	0.071–0.272	0.233–1
cryst dimens/mm	$0.5 \times 0.5 \times 1$	$0.26 \times 0.26 \times 1$	$0.4 \times 0.2 \times 0.2$
cryst habit	colorless cylinder	colorless cylinder	colorless block
$\theta_{\text{max}}/\text{deg}$	25.00	26.49	29.00
no. of rflns: total/unique	12 095/1804	8030/2168	8902/1413
no. of data with $F > 4\sigma(F)$	1487	1789	1143
$R_{\text{int}}$	0.0328	0.0346	0.067
no. of restraints	300	0	0
no. of params	102	85	41
$R(F > 4\sigma(F))$	0.0456	0.0294	0.0351
$R_w(F^2, \text{all data})$	0.1344	0.0753	0.0890
max shift/su	0.001	0.002	0.002
final diff map extremes/ $e \text{\AA}^{-3}$	+0.11, –0.13	+0.81, –0.50	+1.75, –1.69

### Crystal Structure Determination of BMe<sub>3</sub>

Diffraction data were collected for a sample at 95 K. Complete indexing of the diffraction pattern of the sample of BMe<sub>3</sub> described above required two orientation matrices.<sup>16</sup> The relationship between the component orientations could be described with the matrix

$$\begin{pmatrix} -1.00 & -0.03 & 0.00 \\ -0.09 & 1.00 & 0.04 \\ 0.01 & 0.06 & -1.00 \end{pmatrix},$$

which approximates to a 180° rotation about [010]. Since this is a symmetry operation of a monoclinic lattice, the result implies that the sample consisted of two slightly misaligned crystals. Such “twinning” conditions may give rise to refinement difficulties because reflections from different domains partially overlap, but such problems were avoided by simultaneous integration of both components, which ensures that fully and partially overlapping reflections are treated correctly.<sup>17</sup> An absorption correction was applied using the recently written program TWINABS,<sup>18</sup> which is based on the multiscan procedure of Blessing<sup>19</sup> and designed to treat twinned data. Data from both components were used in refinement, the final residuals being only some 0.2% higher than if pure single-component data were used.

The structure was solved by direct methods and refined by full-matrix least squares against  $|F|^2$  using all data (SHELXTL),<sup>20</sup> with anisotropic displacement parameters modeled for the B and C atoms. It was clear from electron density difference maps that the methyl groups were disordered by a 180° rotation about their B–C axes. The relative occupancies were initially refined independently, but later these were modeled with one variable for all three methyl groups after they had converged to common values. The occupancy of the major component (labeled H1A–H1C etc. in the Supporting Information) was 0.577(6).

The orientation of the methyl groups was such that one C–H bond lay in the molecular BC<sub>3</sub> plane, and some distortion from ideal, local C<sub>3v</sub> symmetry was anticipated (see below). The H atom positions were refined subject to the restraint that all in-plane BCH angles were similar. Similarity restraints were also applied to the out-of-plane BCH angles and all 1,2-C–H and 1,3-H···H distances. “Opposite” H atoms attached to the same carbon atom but in different disorder components were constrained to have equal isotropic displacement parameters.

#### *Crystal Structure Determinations of GaMe<sub>3</sub> and TlMe<sub>3</sub>*

Diffraction data were collected for crystals held at 120 K (GaMe<sub>3</sub>) and 150 K (TlMe<sub>3</sub>), and absorption corrections were applied using the program SADABS.<sup>21</sup> The structures were solved by direct methods and refined by full-matrix least squares against  $|F|^2$  using all data (SHELXTL), with anisotropic displacement parameters modeled for the metal and C atoms. The methyl groups were treated as freely rotating rigid groups. Four out of the six independent methyl groups in GaMe<sub>3</sub> were found to be disordered in a fashion similar to that described above for BMe<sub>3</sub>. The relative occupancies were fixed at 0.5:0.5. No attempt was made to model a deviation of the methyl groups from local C<sub>3v</sub> symmetry; the improvement to refinement statistics on introduction of a more flexible model was marginal for BMe<sub>3</sub> and would have been negligible for this compound, where H atom scattering contributes relatively much less to the diffraction pattern.

Refinement and geometric data for all compounds are collected in Tables 1 and 2, respectively. Structural analyses used the program PLATON,<sup>22</sup> and figures were drawn using SHELXTL or CAMERON.<sup>23</sup> The file

CCDC 209601–209603 contains the supplementary crystallographic data for this paper. These data can be obtained free of charge via [www.ccdc.cam.ac.uk/conts/retrieving.html](http://www.ccdc.cam.ac.uk/conts/retrieving.html) (or from the Cambridge Crystallographic Data Centre, 12 Union Road, Cambridge CB2 1EZ, U.K.; fax +44 1223 336033; e-mail [deposit@ccdc.cam.ac.uk](mailto:deposit@ccdc.cam.ac.uk)).

**Table 2.** Observed Bond and Contact Distances (Å) and Angles (deg) in  $\text{MMe}_3$  (M = B, Ga, Tl)<sup>a</sup>

$\text{BMe}_3$ (obsd, $C2/c$ )		$\text{GaMe}_3$ (obsd, $C2/c$ )		$\text{GaMe}_3$ (obsd, $P4_2/n$ )		$\text{TlMe}_3$ (obsd, $P4_2/n$ )	
B1–C1	1.5548(11)	Ga1–C1	1.956(3)	Ga1–C1	1.952(3)	Tl1–C1	2.196(8)
B1–C2	1.5565(11)	Ga1–C2	1.958(3)	Ga1–C2	1.962(2)	Tl1–C2	2.206(8)
B1–C3	1.5541(12)	Ga1–C3	1.968(3)	Ga1–C3	1.958(2)	Tl1–C3	2.216(7)
		Ga1...C5 <sup>b</sup>	3.096(3)	Ga1...C2 <sup>f</sup>	3.149(3)	Tl1...C2 <sup>h</sup>	3.243(8)
		Ga1...C6 <sup>c</sup>	3.512(4)	Ga1...C3 <sup>g</sup>	3.647(3)	Tl1...C3 <sup>i</sup>	3.364(7)
		Ga2–C4	1.964(3)				
		Ga2–C5	1.970(3)				
		Ga2–C6	1.956(3)				
		Ga2...C2 <sup>d</sup>	3.226(3)				
		Ga2...C3 <sup>e</sup>	3.204(3)				
C1–B1–C2	120.06(7)	C1–Ga1–C2	122.02(16)	C1–Ga1–C2	119.72(14)	C1–Tl1–C2	120.7(3)
C1–B1–C3	120.09(7)	C1–Ga1–C3	119.46(16)	C1–Ga1–C3	121.29(14)	C1–Tl1–C3	124.1(3)
C2–B1–C3	119.86(7)	C2–Ga1–C3	118.27(16)	C2–Ga1–C3	118.85(13)	C2–Tl1–C3	115.1(3)
		Ga1...C5 <sup>b</sup> –Ga2 <sup>b</sup>	171.09(18)	Ga1...C2 <sup>f</sup> –Ga1 <sup>f</sup>	167.22(12)	Tl1...C2 <sup>h</sup> –Tl1 <sup>h</sup>	167.8(4)
		Ga1...C6 <sup>c</sup> –Ga2 <sup>c</sup>	120.02(17)	Ga1...C3 <sup>g</sup> –Ga1 <sup>g</sup>	164.67(13)	Tl1...C3 <sup>i</sup> –Tl1 <sup>i</sup>	167.5(4)
		C4–Ga2–C5	120.45(17)				
		C4–Ga2–C6	120.16(18)				
		C5–Ga2–C6	119.39(17)				
		Ga2...C2 <sup>d</sup> –Ga1 <sup>d</sup>	162.14(18)				
		Ga2...C3 <sup>e</sup> –Ga1 <sup>e</sup>	168.71(17)				

<sup>a</sup> Dimensions for the tetragonal phase of  $\text{GaMe}_3$  were calculated from the data in ref 2 (data taken from CCDC 163477). All standard uncertainties were calculated with a full variance–covariance matrix, with the exception of those given in italics. <sup>b</sup>  $-x, y + 1, \frac{1}{2} - z$ . <sup>c</sup>  $\frac{1}{2} - x, \frac{1}{2} + y, \frac{1}{2} - z$ . <sup>d</sup>  $x, y - 1, z$ . <sup>e</sup>  $x, -y, \frac{1}{2} + z$ . <sup>f</sup>  $y, \frac{3}{2} - x, \frac{1}{2} - z$ . <sup>g</sup>  $y - \frac{1}{2}, 1 - x, z - \frac{1}{2}$ . <sup>h</sup>  $\frac{3}{2} - y, x, \frac{1}{2} - z$ . <sup>i</sup>  $1 - y, x - \frac{1}{2}, z - \frac{1}{2}$ .

### Theoretical Methods

Total energy plane-wave DFT calculations were performed using the CASTEP 4.2 simulation code<sup>24</sup> for the compounds  $\text{BMe}_3$ ,  $\text{GaMe}_3$ , and  $\text{InMe}_3$  in ordered layered monoclinic ( $C2/c$ ) and tetragonal ( $P4_2/n$ ) polymorphic forms. Periodic boundary conditions allow the valence electronic wave function to be expanded in terms of a discrete plane-wave basis set (set at 540 eV for  $\text{BMe}_3$  and 500 eV for  $\text{GaMe}_3$  and  $\text{InMe}_3$ ), while the core wave function is described by standard ultrasoft pseudopotentials available with the software package. The symmetry-reduced set of  $k$  points used to sample the reciprocal space were generated using Monkhorst–Pack grids<sup>25</sup> (dimensions  $2 \times 1 \times 1$  and  $1 \times 1 \times 2$  for the monoclinic and tetragonal lattices,

respectively, both generating one  $k$  point in the symmetry-reduced first Brillouin zones). The generalized gradient approximation (GGA) functional PW91<sup>26</sup> was used to model electronic correlation and exchange. Simultaneous optimization of lattice vectors and atomic positions was performed until the convergence criteria were met (maximum energy change per atom  $2 \times 10^{-5}$  eV, maximum RMS displacement  $1.0 \times 10^{-3}$  Å, maximum RMS force 0.05 eV Å<sup>-1</sup>, and maximum RMS stress 0.1 GPa). The starting geometries used for the optimizations of the monoclinic lattice polymorphs were taken from the experimental structure determination of BMe<sub>3</sub> reported in this paper, with the boron atoms simply replaced by gallium or indium to generate input coordinates for the other two structures. The tetragonal lattice atomic coordinates and cell vectors for the BMe<sub>3</sub> and InMe<sub>3</sub> structures originated from Blake's InMe<sub>3</sub> X-ray structure determination;<sup>4</sup> calculations on GaMe<sub>3</sub> used Mitzel's data<sup>2</sup> on the tetragonal polymorph as the starting point (as this structure is the most directly comparable with the others in our series).

The Supporting Information contains tables of crystallographic data for BMe<sub>3</sub>, GaMe<sub>3</sub>, and TlMe<sub>3</sub> (also deposited with the CCDC, as described above) and tables of optimized theoretical coordinates for polymorphs of BMe<sub>3</sub>, GaMe<sub>3</sub>, and InMe<sub>3</sub>.

## Results and Discussion

Under ambient conditions, the trimethyl derivatives of the group 13 elements range from a gas (BMe<sub>3</sub>), through a liquid (AlMe<sub>3</sub> and GaMe<sub>3</sub>), to a low-melting solid (InMe<sub>3</sub> and TlMe<sub>3</sub>).<sup>27</sup> On the evidence of mass and vibrational spectroscopic and electron diffraction measurements, the vapors of all but the aluminum compound consist of monomeric MMe<sub>3</sub> molecules (M = B, Ga, In, Tl), each with a trigonal-planar MC<sub>3</sub> skeleton and more or less freely rotating methyl groups.<sup>9,11,13,28-31</sup> In contrast, the analogous aluminum species, AlMe<sub>3</sub>, is found in appreciable concentrations only at elevated temperatures and/or low pressures,<sup>32,33</sup> otherwise, the dimer Me<sub>2</sub>Al(μ-Me)<sub>2</sub>AlMe<sub>2</sub> prevails throughout the condensed and vapor states.<sup>6</sup> Increasing the atomic number of the group 13 element results in an overall rise in melting and boiling points consistent with the expected strengthening of van der Waals interactions. That the pattern is far from regular, however, is evidenced by the following melting points (in K):<sup>27</sup> BMe<sub>3</sub>, 112; AlMe<sub>3</sub>, 288; GaMe<sub>3</sub>, 257; InMe<sub>3</sub>, 362; TlMe<sub>3</sub>, 312. To what extent the implied cohesive energies of the crystal reflect differences of structure and/or variations in the type or degree of the intermolecular interactions — possibly including so-called “agostic” interactions<sup>34</sup> — is not possible to judge on the evidence available to date. Previous studies involving X-ray crystallography,<sup>1-5</sup> gas electron diffraction,<sup>28-30</sup> and vibrational spectroscopy<sup>4,11,13</sup> argue that perturbation of the MMe<sub>3</sub> units in the crystal is quite modest, with the sole exception of M = Al, for which the dimer Me<sub>2</sub>Al(μ-Me)<sub>2</sub>AlMe<sub>2</sub> holds sway (but is itself subject to relatively little change with the transition from the vapor to the crystalline state<sup>6</sup>). One or two of these studies have also alluded to the possibility of polymorphism, for example in the case of InMe<sub>3</sub>.<sup>3,4</sup> The aims of the present study have been to enlarge on knowledge of the



crystal structures of these compounds and of the secondary interactions they reveal and to explore the possibilities of polymorphism, partly by experiment (in the case of GaMe<sub>3</sub>) but, more widely, by plane wave DFT analysis.

### *Trimethylboron*

The boron-to-carbon distances in BMe<sub>3</sub> are equal within error, and the BC<sub>3</sub> framework adopts the expected  $D_{3h}$  symmetry (Figure 1). The most closely related crystal structure in the literature is that of triethylboron, BEt<sub>3</sub>; the B–C distances in that compound lie around 1.573(1) Å.<sup>35</sup> The corresponding distance in BMe<sub>3</sub> is 1.555(1) Å, but a riding analysis<sup>36</sup> suggests that this difference is probably owed to the relatively high librational motion of the methyl groups at the temperature used for data collection (95 K), which is only 17 K below the melting point. In this context, it is perhaps significant that the B–C distance in the gaseous BMe<sub>3</sub> molecule (determined by electron diffraction) is reported to be 1.5783(11) Å.<sup>28</sup>

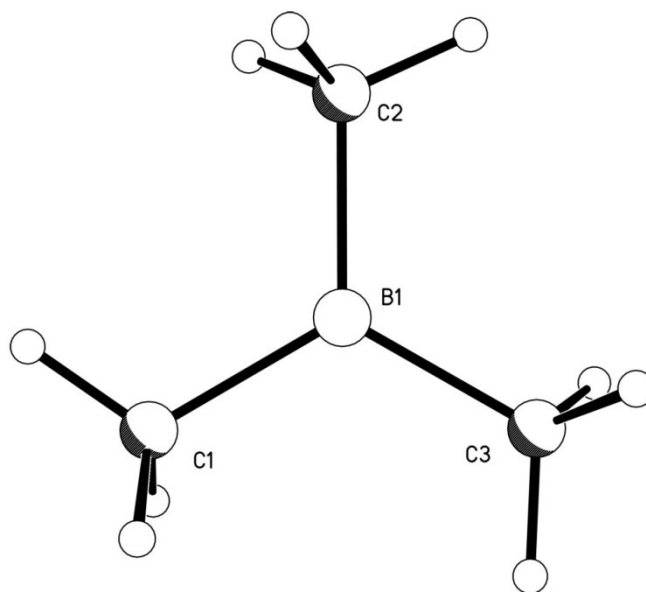


**Figure 1.** Crystal structure of BMe<sub>3</sub> viewed along the crystallographic *c* direction. The molecules are related either by lattice translations or *C*-centering operations. The minor disorder component has been omitted for clarity. Displacement ellipsoids enclose 50% probability surfaces.

The BCC angle in BEt<sub>3</sub> would be expected, on the basis of simple predictions using VSEPR theory, for example, to be close to 109.5°, and the most remarkable feature of the structure of this compound is the rather

large BCC angle, reported to be  $118.9(2)^\circ$ . A similar effect has recently been observed in  $\text{GaEt}_3$ .<sup>2</sup> The reason for this deviation has been ascribed to hyperconjugation between the out-of-plane  $\text{CH}_2$  bonds and the vacant p orbital on the central group 13 atom. The methyl groups in  $\text{BMe}_3$  are disordered by a  $180^\circ$  rotation about the B–C vector, each component containing one CH bond in the  $\text{BC}_3$  plane. The ab initio optimized crystal structure of an ordered model of  $\text{BMe}_3$  (see below) revealed that the average in-plane BCH angle was  $115^\circ$ , whereas the average out-of-plane BCH angle was  $110^\circ$ . Scattering from the H atoms in  $\text{BMe}_3$  contributes some 28% to  $F(000)$ , giving them a significant influence on data fitting, and it seemed possible that a deviation from ideal tetrahedral geometry about the carbon atoms in  $\text{BMe}_3$  might be detectable, despite the disorder. Restrained refinement of a model in which the BCH angles were allowed to vary revealed a trend rather similar to that observed in the BCC angles in  $\text{BEt}_3$ , with the in-plane BCH angles averaging  $116^\circ$ , compared with  $109^\circ$  for the out-of-plane BCH angles, in very good agreement with the theoretical results. The standard uncertainties of these quantities (excluding the effects of restraints) fall in the range  $1.1\text{--}1.8^\circ$ . This places the difference on the limit of statistical significance. A refinement model in which the methyl groups were constrained to adopt perfect  $C_{3v}$  symmetry yielded a conventional  $R$  factor of 5.2% (48 parameters), compared with 4.5% for the model described here (102 parameters). For what it is worth, the Hamilton test<sup>37</sup> using weighted residuals implies that the improvement is significant.

In the crystal structure of  $\text{BMe}_3$  the molecules pack in layers which stack along the  $c$  direction (Figure 2). The boron and hydrogen atoms respectively carry small positive and negative charges, and the boron atoms lie between methyl groups in neighboring layers. The shortest intermolecular  $\text{B}\cdots\text{H}$  contact is  $3.04\text{ \AA}$ , which is well beyond the sum of the van der Waals radii of B and H ( $2.83\text{ \AA}$ ),<sup>38</sup> a finding consistent no doubt with the high volatility of trimethylboron. The arrangement of the molecules within the layers (Figure 1) resembles a close-packed array.

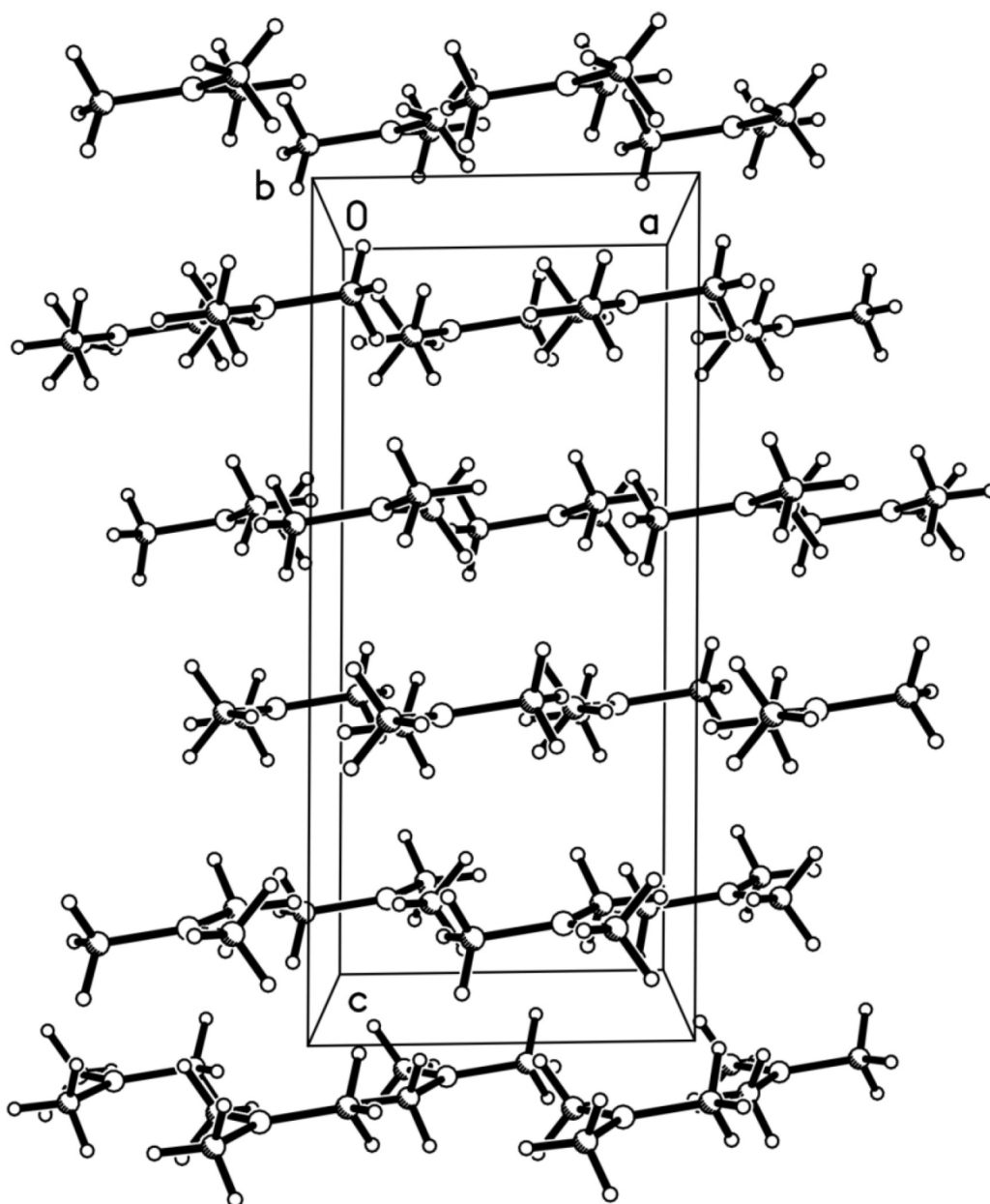


**Figure 2.** Formation of layers in the crystal structure of BMe<sub>3</sub> (view along the crystallographic *b* direction). Packing within the layers is illustrated in Figure 1.

#### *Trimethylgallium and Trimethylthallium*

Trimethylboron is unique among the group 13 trimethyls in showing no significant association in the solid state. Trimethylaluminum exists as a methyl-bridged dimer both in the solid state and in the gas phase. Although such behavior is not observed for Ga, In, and Tl, it has long been clear that these trimethyls are also associated via secondary metal···methyl contacts in the solid state. The melting points of GaMe<sub>3</sub> (257 K),

InMe<sub>3</sub> (362 K), and TlMe<sub>3</sub> (312 K) alternate along the series, and are all significantly higher than that of BMe<sub>3</sub> (112 K), partly as a result of these interactions.

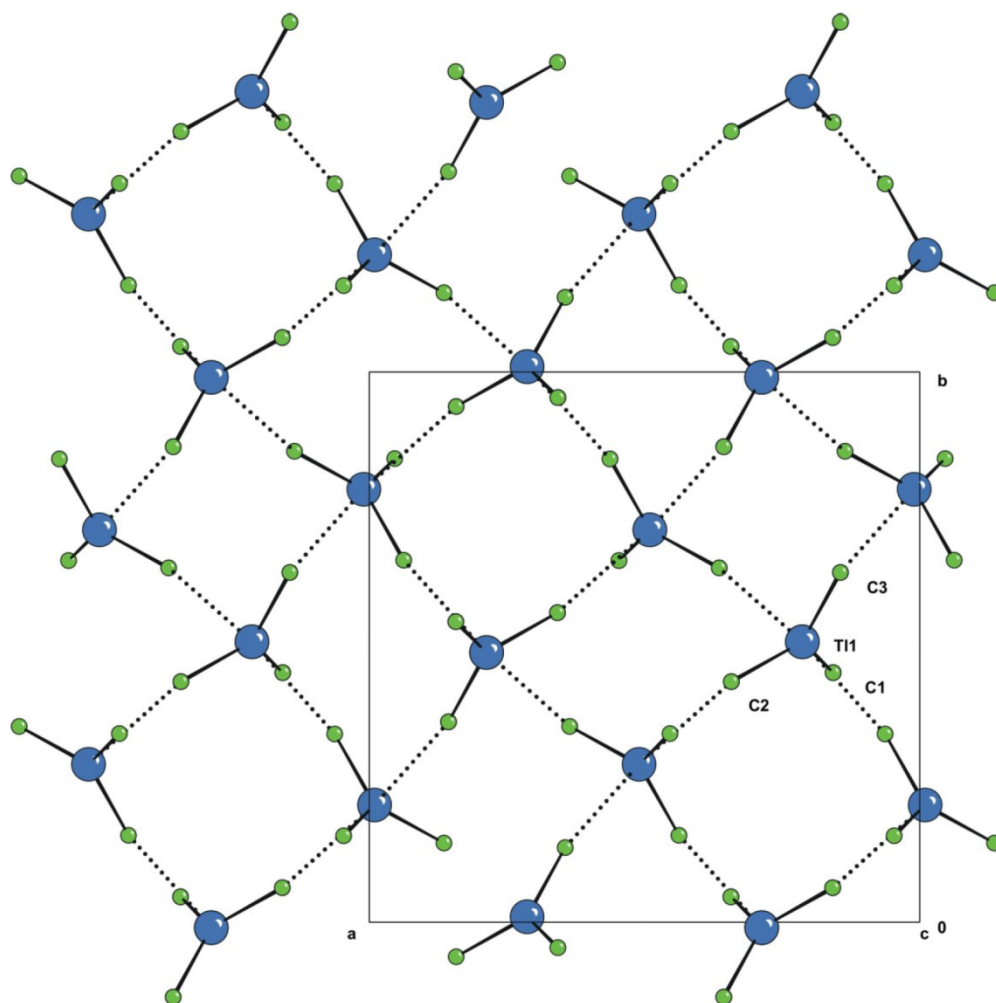


**Figure 3.** Structure of TlMe<sub>3</sub> projected onto (001), showing methyl bridge formation. Hydrogen atoms have been omitted for clarity. Ellipsoids enclose 50% probability surfaces.

Trimethylindium has the highest melting point of the trimethyl derivatives formed by the three heaviest group 13 metals, and it might be inferred from this that it exhibits the strongest degree of association in the solid state. Its crystal structure, first investigated by Amma and Rundle in 1958<sup>3</sup> and then again by Blake and Cradock in 1990,<sup>4</sup> is characterized by the formation of pseudo-tetramers (Rundle's term) which consist of four InMe<sub>3</sub> molecules connected via long In···methyl bridges (In···C = 3.083(12) Å). These are disposed about a crystallographic 4̄ site, forming a flattened tetrahedron. Longer In···methyl bridges (In···C = 3.558(15) Å)

connect the tetramers. Projections of this structure along [001] (Figure 3 shows the isostructural Tl derivative in this projection) can beguile one into thinking that this structure is a two-dimensional network. In fact, it is three-dimensional, consisting of two mutually exclusive networks which are interlaced by means of a 4-fold screw axis.<sup>3</sup>

An atoms-in-molecules analysis<sup>39</sup> on the related gallium system has shown that the critical point in the metal···methyl bridge region occurs along the Ga···C vector, implying that this is not an agostic interaction.<sup>2</sup> In the following sections we discuss intermolecular interactions in terms of metal-to-carbon distances partly for this reason, but also because H atom positions have not been determined very precisely and because they are consistent with the contemporary literature in this area.

The crystal structure of TlMe<sub>3</sub> was investigated using photographic methods by Sheldrick and Sheldrick in 1970.<sup>5</sup> Our data set establishes the structural parameters to greater precision than was possible in that study, although the conclusions are unchanged. TlMe<sub>3</sub> adopts the InMe<sub>3</sub> structure (Figure 3), but there is a much smaller difference between the lengths of the short and long secondary metal to methyl contacts: the Tl···C distances are 3.243(8) and 3.364(7) Å within and between the tetramers, respectively. The primary Tl–C bond distances, averaging 2.206(8) Å, are identical with those in the gaseous molecule (2.206(3) Å), as gauged by electron diffraction.<sup>30</sup>

Very recently Mitzel et al. reported a crystal structure of GaMe<sub>3</sub> which is isostructural with that of InMe<sub>3</sub>.<sup>2</sup> In this tetragonal phase both the Ga···methyl contacts which form the tetramers and those between the tetramers are slightly longer than in InMe<sub>3</sub> (3.134 and 3.647 Å, respectively). This phase was obtained by cooling a sample of GaMe<sub>3</sub> through its melting point, but crystal growth by laser-assisted zone refinement yielded a new polymorph of GaMe<sub>3</sub>, which is *C*-centered monoclinic. The structure contains two crystallographically independent molecules, both of which adopt the expected trigonal-planar geometry in the primary coordination sphere.

The length of the *b* axis of the unit cell of the monoclinic phase is similar to that of the *c* axis of the tetragonal phase, and when projected along these directions the structures bear a close resemblance to each other. However, the tetramers which characterize the tetragonal phase of GaMe<sub>3</sub> are replaced in the monoclinic phase by a polymer. The two crystallographically independent molecules alternate along chains with methyl···Ga contacts of 3.226(3) and 3.204(3) Å formed above and below the planes of the molecules containing Ga2. Shorter contacts of 3.096(3) Å made to Ga1 serve to link the chains together into a ladderlike array (Figure 4). Long contacts measuring 3.512(4) Å are formed between the ladders, completing the trigonal-bipyramidal coordination about Ga1. In the tetragonal forms of MMe<sub>3</sub> (M = Ga, In, Tl) the angles subtended at bridging carbon atoms fall in the range 160–170°. This trend is also followed in the structure of monoclinic GaMe<sub>3</sub>, except in the case of the long interconnecting methyl bridge (C6), where the angle is 120.02(17)°.

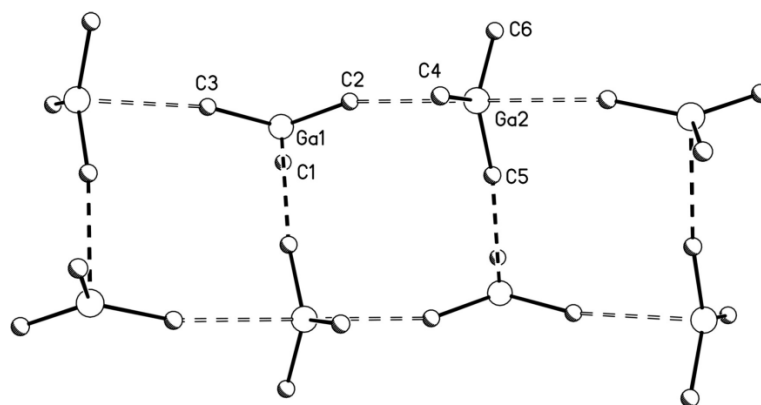


**Figure 4.** Pseudo-polymer formed in the crystal structure of the monoclinic polymorph of  $\text{GaMe}_3$ . The heavy dotted lines are short contacts of 3.096(3) Å; the light dotted lines are longer contacts of 3.204(3) and 3.226(3) Å. The ellipsoids enclose 50% probability surfaces; H atoms have been omitted for clarity.

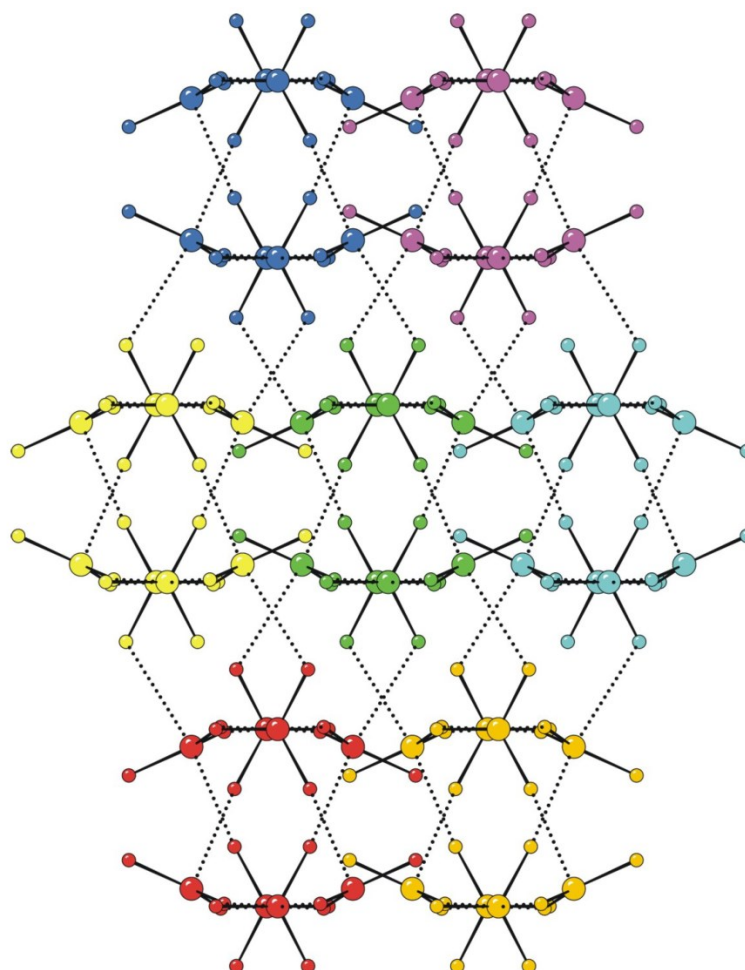


**Figure 5.** Structure of monoclinic  $\text{GaMe}_3$  projected onto (001). The polymers shown in Figure 5 pass into the page, and different polymers have been shown in different colors. Domains of short (between 3.0 and 3.3 Å) and long (3.512 Å)  $\text{Ga}\cdots\text{C}$  contacts are indicated by the letters S and L, respectively.

Figure 5 shows a projection of the monoclinic structure along the  $c$  direction; it should be compared with Figure 6, which shows the structure of  $\text{TlMe}_3$  (which can be taken to be representative of all the tetragonal  $\text{MMe}_3$  phases) projected perpendicular to the (110) plane. These rather similar packing arrangements are related by a shift in the relative positions of layers containing the short contacts. The pattern of contacts in the two phases is represented schematically in Figure 7, which is intended to illustrate the transition from a structure consisting of two independent three-dimensional networks in the tetragonal phases of  $\text{MMe}_3$  ( $\text{M} = \text{Ga}, \text{In}, \text{Tl}$ ) to a single three-dimensional network in the monoclinic phase of  $\text{GaMe}_3$ .

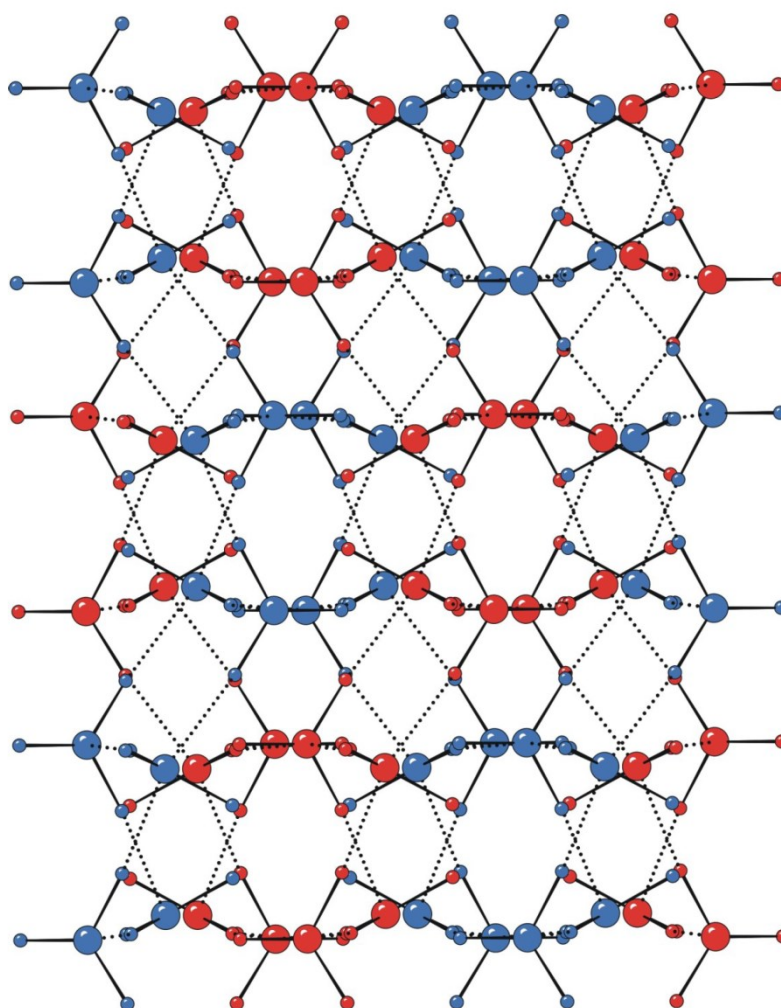


**Figure 6.** Structure of  $\text{TlMe}_3$  projected onto (110). The two different three-dimensional networks are shown in blue and red. Domains of shorter (3.243 Å) and longer (3.364 Å)  $\text{Tl}\cdots\text{C}$  contacts are indicated by the letters S and L, respectively. Isostructural tetragonal polymorphs are known for  $\text{GaMe}_3$  (in which the short and long contacts are 3.149(3) and 3.647(3) Å, respectively) and  $\text{InMe}_3$  (contact distances 3.083(12) and 3.558(15) Å).

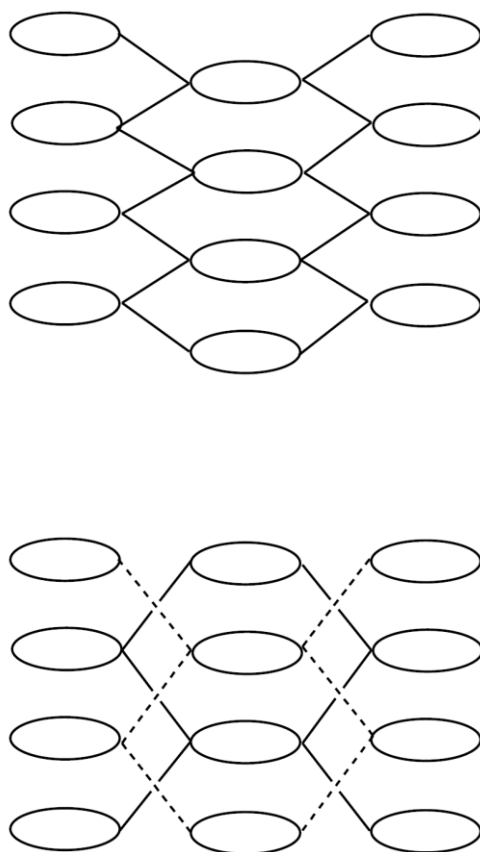


**Figure 7.** Schematic representations of Figure 5 (top, monoclinic GaMe<sub>3</sub>) and Figure 6 (bottom, TlMe<sub>3</sub>) showing the formation of two independent networks following displacement of layers. In the top part of the figure, the ellipses represent polymers passing into the plane of the paper. In the bottom part of the figure, they represent columns of tetramers.

#### *Ab Initio Calculations of Polymorphs of Group 13 Trimethyls*

There is some evidence in the literature that InMe<sub>3</sub> may exist in at least two different polymorphic forms. Blake and Cradock<sup>4</sup> refer to an alternative form of InMe<sub>3</sub>, which they describe as being less volatile, and more stable, than the tetragonal form. However, a careful variable-temperature X-ray diffraction study between 273 and 113 K did not reveal any new phases. In their study of the same compound, Amma and Rundle<sup>3</sup> noted that, in addition to the tetragonal phase, a less common, *less* stable, pseudo-hexagonal (more likely triclinic) form was found to exist. This conclusion was based on crystal morphology, and no diffraction data have ever been collected on this form of InMe<sub>3</sub>. However, the reduced cell dimensions of BMe<sub>3</sub> are pseudohexagonal, with  $a = b = 6.319 \text{ \AA}$ ,  $c = 14.224 \text{ \AA}$ ,  $\alpha = \beta = 90.55^\circ$ , and  $\gamma = 119.70^\circ$ , and it is possible that the less stable phase is closely related to the structure of BMe<sub>3</sub> described here. The  $ab$  plane of this pseudo-hexagonal lattice



is evident in Figure 1, perhaps most clearly by treating each B atom as a lattice point, though this would not be the conventional choice of origin.

Polymorphism is a very common phenomenon, and it seems perfectly reasonable that the group 13 trimethyls should be as susceptible to it as any other class of compound. Indeed, as described above, we have observed it for GaMe<sub>3</sub>. However, our new polymorph falls into the same structural category, being characterized by long methyl bridges, as the known tetragonal structures; whereas the latter are pseudo-tetrameric, the new polymorph is pseudo-polymeric, and the energy difference between the two forms is presumably small. The observations by previous workers concerning trimethylindium suggest that it may be possible to observe transitions *between* structural types by varying the conditions of temperature and/or pressure. With this in mind, we have investigated the energetic differences between layered and pseudo-tetrameric polymorphs of BMe<sub>3</sub>, GaMe<sub>3</sub>, and InMe<sub>3</sub> using plane wave density functional theory (DFT). Previous work in our research groups has shown plane wave DFT calculations to be a very successful and useful tool to investigate (a) polymorphic transitions which occur in small organic systems under the application of high pressure,<sup>40,41</sup> (b) the properties of hydrogen bonds,<sup>42</sup> and (c) crystal disorder in PbCp<sub>2</sub>.<sup>43</sup> Our calculations on GaMe<sub>3</sub> used Mitzel's coordinates for the tetragonal polymorph, as this is most directly comparable with InMe<sub>3</sub>.

The results of the calculations are shown in Table 3. Bond and contact distances tend to be overestimated at this level of theory, an effect which carries through to the unit cell dimensions, which are also overestimated. Of course, the C–H bond lengths are all ca. 0.1 Å longer than those obtained experimentally, but most of this disagreement arises from the systematic shortening of these parameters when derived from X-ray data. Nevertheless, both the present results and those of our previous work in this area show that structural trends (for example, in a set of bond lengths within a structure) are reliably reproduced. So too are relative energies. In all three cases, the lower energy structure corresponds to the experimentally observed polymorph. The calculated tetragonal polymorph of BMe<sub>3</sub> has a very long B···C “contact” of 3.715 Å, exceeding even the related distances in either GaMe<sub>3</sub> or InMe<sub>3</sub>. Modeling suggests that shortening this contact to a more reasonable distance between 3.0 and 3.3 Å begins to incur repulsive H···H interactions between methyl groups of less than twice the van der Waals radius of H (2.4 Å). This does not occur in the heavy-atom derivatives because of their longer metal-to-carbon bonds. Conversely, the short B–C bond enables the electron deficiency of the boron to be relieved by hyperconjugation between the empty 2p orbital on the boron and the out-of-plane C–H bonds of the methyl groups, a circumstance supported both experimentally and by the results of these calculations (see above). Presumably the reverse of this argument explains the preference for the methyl-bridged structures by the heavier group 13 trimethyls. As the experimental structure of GaEt<sub>3</sub> shows, hyperconjugation is also possible in these systems, although it is notable that the shortest calculated interplanar M···C distances in the *C2/c* polymorphs become shorter along the series B > Ga > In. There is also a tendency along this series for the methyl groups to rotate about the C–metal bond away from the conformation described above for BMe<sub>3</sub>.

**Table 3.** Calculated Solid State Structural Parameters for Polymorphs of  $\text{MMe}_3$  ( $\text{M} = \text{B}, \text{Ga}, \text{In}$ )<sup>a</sup>

	$\text{BMe}_3$			$\text{GaMe}_3$			$\text{InMe}_3$		
model	obsd $C2/c$	calcd $C2/c$	calcd $P4_2/n$	calcd $C2/c$	obsd $P4_2/n^2$	calcd $P4_2/n$	calcd $C2/c$	obsd $P4_2/n^4$	calcd $P4_2/n$
$a/\text{\AA}$	6.3473 (9)	6.6648	13.0536	7.3159	12.953 2(3)	13.4392	7.4839	13.216 6(11)	14.0377
$b/\text{\AA}$	10.928 4(16)	11.2908	13.0536	12.1062	12.953 2(3)	13.4392	12.5123	13.216 6(11)	14.0377
$c/\text{\AA}$	14.224 (2)	14.6057	6.371433	14.7211	6.2588 (1)	6.4588	14.6060	6.4039 (9)	7.1097
$\beta/\text{deg}$	91.099 (3)	90.002	90.0	88.536	90	90	88.973	90	90
$\text{M1}\cdots\text{C1}/\text{\AA}$	1.5548 (11)	1.554	1.556	1.971	1.952( 3)	1.973	2.192	2.136( 13)	2.180
$\text{M1}\cdots\text{C2}/\text{\AA}$	1.5565 (11)	1.558	1.556	1.970	1.962( 2)	1.985	2.185	2.179( 12)	2.211
$\text{M1}\cdots\text{C3}/\text{\AA}$	1.5541 (12)	1.555	1.554	1.972	1.958( 3)	1.977	2.190	2.121( 14)	2.189
$\text{M1}\cdots\text{C2}^c/\text{\AA}_b$			3.715		3.149( 3)	3.266		3.083( 12)	3.181
$\text{M1}\cdots\text{C3}^c/\text{\AA}_b$			4.009		3.647( 3)	3.848		3.558( 15)	4.091
$\text{C1}\cdots\text{M1}\cdots\text{C2}/\text{deg}$	120.06 (7)	119.5	119.6	119.2	119.72 (14)	120.4	119.0	119.7( 5)	118.2
$\text{C2}\cdots\text{M1}\cdots\text{C3}/\text{deg}$	120.09 (7)	120.0	121.5	120.3	121.29 (14)	119.1	119.8	116.8( 5)	118.3
$\text{C1}\cdots\text{M1}\cdots\text{C3}/\text{deg}$	119.86 (7)	120.5	118.9	120.5	118.85 (13)	120.3	121.1	123.5( 5)	122.9
$\text{M1}\cdots\text{C2}^c\cdots\text{M1}^c/\text{deg}^b$			170.0		167.23 (12)	168.9		168.1( 6)	167.8
$\text{M1}\cdots\text{C3}^c\cdots\text{M1}^c/\text{deg}^b$			164.2		164.67 (13)	162.8		166.2( 6)	164.0
$\text{M1}\cdots\text{C1}^c/\text{deg}^c$	3.7908 (13)	3.826		3.758			3.525		
$E_{\text{tot}}/\text{eV}$		-5547.36 9 2869	-5547.22 4 9200	-21 406.5 43 6047		-21 406.8 41 8865	-17 435.0 88 4853		-17 435.9 51 7724
$E_{\text{rel}}/\text{kJ mol}^{-1}$		0	+1.7	+3.6		0.0	+10.4		0.0

<sup>a</sup> The structures in  $C2/c$  are analogous to the observed layered structure of  $\text{BMe}_3$  (this should not be confused with the monoclinic polymorph of  $\text{GaMe}_3$ , which is also described in this paper). Structures in  $P4_2/n$  are based on the pseudo-tetrameric structure of  $\text{InMe}_3$ . All structures have  $Z = 8$  and  $\alpha = \gamma = 90^\circ$ .  $E_{\text{tot}}$  refers to one unit cell.  $E_{\text{rel}}$  is the energy per molecule relative to the lower energy polymorph, which is given the value  $E_{\text{rel}} = 0$ . <sup>b</sup> Tetragonal structures only; these are the distances and angles involving the methyl bridges. <sup>c</sup> Monoclinic structures only; this is the shortest interplanar  $\text{M}\cdots\text{C}$  distance. Primes refer to symmetry-equivalent atoms; refer to Table 2 for full details.

Mitzel et al. performed calculations at the MP2/TZVP level on an isolated pair of  $\text{GaMe}_3$  molecules in which a  $\text{Ga}\cdots\text{C}$  bridging interaction measuring 3.206 Å was found to have an energy of 11.4 kJ mol<sup>-1</sup>. Of this, only 3.4 kJ mol<sup>-1</sup> was ascribable to electrostatic forces; the remainder arose from a dispersion interaction (7.5 kJ mol<sup>-1</sup>), an ionic correlation contribution (4.2 kJ mol<sup>-1</sup>, from a reduction in intramolecular correlation on approach of

two molecules), and a negative repulsive term ( $-3.8 \text{ kJ mol}^{-1}$ ).<sup>2</sup> The total interaction energy is rather similar to that of a weak hydrogen bond. The energy differences between polymorphs are of the same order of magnitude as the terms given above. The two optimized structures of  $\text{BMe}_3$  both consist of very weakly interacting molecules, and not surprisingly, the energy difference between them is small. The corresponding energy difference between the polymorphs of  $\text{InMe}_3$  is greater than for  $\text{GaMe}_3$ , consistent with the shorter bridges formed in  $\text{InMe}_3$ . Enthalpy differences between real polymorphs usually fall in the range  $0\text{--}10 \text{ kJ mol}^{-1}$  and probably do not exceed  $25 \text{ kJ mol}^{-1}$ .<sup>7</sup> Therefore, the results of these calculations show it to be quite possible that the unstable phase of  $\text{InMe}_3$  observed by Amma and Rundle had the  $\text{BMe}_3$  structure.

### *Distortions Caused by Methyl Bridging*

When an atom forms a strong contact, any other bonds that it forms are generally weakened as a result. In our structure of  $\text{GaMe}_3$  the primary Ga–C distances span the range  $1.956(3)\text{--}1.970(3) \text{ \AA}$ ; the average distance in the gaseous molecule, deduced by electron diffraction,<sup>29</sup> is  $1.967(2) \text{ \AA}$ . The carbon atom involved in the shortest intermolecular contact ( $\text{C5}\cdots\text{Ga1} = 3.096(3) \text{ \AA}$ ) also makes the longest primary C–Ga bond, but there is no discernible relationship between the other bond and contact lengths in the structure. The calculations on tetragonal  $\text{InMe}_3$  show that the In–C bond length involving the carbon atom making the stronger secondary contact is  $0.03 \text{ \AA}$  longer than the bond involving the carbon atom, which is not involved in bridging. The relative lengthening of the In–C bond involving the carbon that makes the longer contact is much less, viz.  $0.009 \text{ \AA}$ .<sup>44</sup> The corresponding figures for tetragonal  $\text{GaMe}_3$  are  $0.012$  and  $0.004 \text{ \AA}$ , in excellent agreement with the experimental values. The relative lengthening of the bond involving the more strongly bridging methyl group which has been discussed by several authors<sup>2-5</sup> thus appears to be a genuine effect, even though the differences observed crystallographically tend to teeter on the brink of statistical insignificance.

Bond angles are somewhat “softer” interactions than bond lengths, and all structures exhibit C–M–C angles which differ from  $120^\circ$ . Where a significant deviation occurs, the largest bond angle is invariably the one not involving the carbon atom making the stronger intermolecular contact. There is no deviation from planarity in the molecular  $\text{MC}_3$  unit in any of the crystal structures. In contrast, the very strong bridging contacts established in monomeric aluminum derivatives containing bulky groups, such as  $\text{Al}(\text{CH}_2\text{Ph})_3$ <sup>45</sup> and  $\text{Al-}t\text{-Bu}_3$ ,<sup>46</sup> have been observed to lift the Al atom out of the plane formed by the three directly bound carbon atoms by up to  $0.4 \text{ \AA}$ .

## References

- [1] Vranka, R. G.; Amma, E. L. *J. Am. Chem. Soc.* **1967**, *89*, 3121. Byram, S. K.; Fawcett, J. K.; Nyberg, S. C.; O'Brien, R. J. *J. Chem. Soc. D* **1970**, 16. Huffman, J. C.; Streib, W. E. *J. Chem. Soc. D* **1971**, 911.
- [2] Mitzel, N. W.; Lustig, C.; Berger, R. J. F.; Runeberg, N. *Angew. Chem., Int. Ed.* **2002**, *41*, 2519.
- [3] Amma, E. L.; Rundle, R. E. *J. Am. Chem. Soc.* **1958**, *80*, 4141.
- [4] Blake, A. J.; Cradock, S. *J. Chem. Soc., Dalton Trans.* **1990**, 2393.
- [5] Sheldrick, G. M.; Sheldrick, W. S. *J. Chem. Soc. A* **1970**, 28.
- [6] McGrady, G. S.; Turner, J. F. C.; Ibberson, R. M.; Prager, M. *Organometallics* **2000**, *19*, 4398.
- [7] Bernstein, J. *Polymorphism in Molecular Crystals*; Clarendon Press: Oxford, U.K., 2002.
- [8] Köster, R. *Justus Liebigs Ann. Chem.* **1958**, *618*, 31.
- [9] Woodward, L. A.; Hall, J. R.; Dixon, R. N.; Sheppard, N. *Spectrochim. Acta* **1959**, *15*, 249.
- [10] Gaines, D. F.; Borlin, J.; Fody, E. P. *Inorg. Synth.* **1974**, *15*, 203.
- [11] McKean, D. C.; McQuillan, G. P.; Duncan, J. L.; Shephard, N.; Munro, B.; Fawcett, V.; Edwards, H. G. M. *Spectrochim. Acta* **1987**, *43A*, 1405.
- [12] Gilman, H.; Jones, R. G. *J. Am. Chem. Soc.* **1946**, *68*, 517.
- [13] Schwerdtfeger, P.; Bowmaker, G. A.; Boyd, P. D. W.; Ware, D. C.; Brothers, P. J.; Nielson, A. J. *Organometallics* **1990**, *9*, 504. Johnson, E. M. D.Phil. Thesis, University of Oxford, 1971.
- [14] Cosier, J.; Glazer, A. M. *J. Appl. Crystallogr.* **1986**, *19*, 105.
- [15] Boese, R.; Nussbaumer, M. In *Correlations, Transformations, and Interactions in Organic Crystal Chemistry*; Jones, D. W., Katrusiak, A., Eds.; IUCr Crystallographic Symposia 7; Oxford University Press: Oxford, U.K., 1994; p 20.
- [16] Sparks, R. A. GEMINI: Program for Indexing X-ray Diffraction Patterns Derived from Multiple or Twinned Crystals; Bruker-AXS, Madison, WI, 2000.
- [17] SAINT, version 6.33; Bruker-Nonius, Madison, WI, 2002.

- [18] Sheldrick, G. M. TWINABS: Program for Performing Absorption Corrections to X-ray Diffraction Patterns Collected from Non-Merohedrally Twinned and Multiple Crystals; University of Göttingen, Göttingen, Germany, 2002.
- [19] Blessing, R. H. *Acta Crystallogr.* **1995**, *A51*, 33.
- [20] Sheldrick, G. M. SHELXTL: Suite of Programs for Crystal Structure Analysis, Incorporating Structure Solution (XS), Least-Squares Refinement (XL), and Graphics (XP); University of Göttingen, Göttingen, Germany, 2001.
- [21] Sheldrick, G. M. SADABS: Program for Performing Absorption Corrections to Single-Crystal X-ray Diffraction Patterns; University of Göttingen, Göttingen, Germany, 2002.
- [22] Spek, A. L. PLATON: A Multipurpose Crystallographic Tool; Utrecht University, Utrecht, The Netherlands, 2002. PC version: Farrugia, L. J. *J. Appl. Crystallogr.* **1999**, *32*, 837.
- [23] Watkin, D. J.; Pearce, L.; Prout, C. K. CAMERON—A Molecular Graphics Package; Chemical Crystallography Laboratory, University of Oxford, Oxford, U.K., 1993.
- [24] Payne, M. C.; Teter, M. P.; Allan, D. C.; Arias, T. A.; Joannopoulos, J. D. *Rev. Mod. Phys.* **1992**, *64*, 1045. CASTEP 4.2 Academic version, licensed under the UKCP-MSI agreement, 1999.
- [25] Monkhorst, H. J.; Pack, J. D. *Phys. Rev. B* **1976**, *13*, 5188.
- [26] Perdew, J. P.; Chevary, J. A.; Vosko, S. H.; Jackson, K. A.; Pederson, M. R.; Singh, D. J.; Fiolhais, C. *Phys. Rev. B* **1992**, *46*, 5571.
- [27] Starowieyski, K. In *Chemistry of Aluminium, Gallium, Indium and Thallium*; Downs, A. J., Ed.; Blackie Academic and Professional: Glasgow, U.K., 1993; p 339. Macintyre, J. E., Ed. *Dictionary of Organometallic Compounds*, 2nd ed.; Chapman and Hall: London, U.K.; 1995.
- [28] Bartell, L. S.; Carroll, B. L. *J. Chem. Phys.* **1965**, *42*, 3076.
- [29] Beagley, B.; Schmidling, D. G.; Steer, I. A. *J. Mol. Struct.* **1974**, *21*, 437.
- [30] Fjeldberg, T.; Haaland, A.; Seip, R.; Shen, Q.; Weidlein, J. *Acta Chem. Scand., Ser. A* **1982**, *36*, 495.
- [31] Hall, J. R.; Woodward, L. A.; Ebsworth, E. A. V. *Spectrochim. Acta* **1964**, *20*, 1249.
- [32] Almenningen, A.; Halvorsen, S.; Haaland, A. *Acta Chem. Scand.* **1971**, *25*, 1937.
- [33] Atiya, G. A.; Grady, A. S.; Russell, D. K.; Claxton, T. A. *Spectrochim. Acta* **1991**, *47A*, 467. Kvisle, S.; Rytter, E. *Spectrochim. Acta* **1984**, *40A*, 939.

- [34] Brookhart, M.; Green, M. L. H.; Wong, L.-L. *Prog. Inorg. Chem.* **1988**, *36*, 1. Scherer, W.; McGrady, G. S. Submitted for publication in *Angew. Chem., Int. Ed.*
- [35] Boese, R.; Bläser, D.; Niederprüm, N.; Nüsse, M.; Brett, W. A.; Schleyer, P. v. R.; Bühl, M.; van Eikema Hommes, N. J. R. *Angew. Chem., Int. Ed. Engl.* **1992**, *31*, 314.
- [36] Johnson, C. K. In *Crystallographic Computing, Proceedings of the International Summer School*; Munksgaard: Copenhagen, Denmark, 1970; pp 220–226.
- [37] Hamilton, W. C. *Acta Crystallogr.* **1965**, *18*, 502.
- [38] Bondi, A. *J. Phys. Chem.* **1964**, *68*, 441.
- [39] Bader, R. F. W. *Atoms in Molecules: A Quantum Theory*; Clarendon Press: Oxford, U.K., 1994.
- [40] Allan, D. R.; Clark, S. J.; Ibberson, R. M.; Parsons, S.; Pulham, C. R.; Sawyer, L. *Chem. Commun.* **1999**, 751.
- [41] Allan, D. R.; Clark, S. J.; Dawson, A.; McGregor, P. A.; Parsons, S. *Acta Crystallogr.* **2002**, *B58*, 1018.
- [42] (a) Morrison, C. A.; Siddick, M. M. *Chem. Eur. J.*, in press. (b) Wilson, C. C.; Morrison, C. A. *Chem. Phys. Lett.* **2002**, *362*, 85.
- [43] Morrison, C. A.; Wright, D. S.; Layfield, R. A. *J. Am. Chem. Soc.* **2002**, *124*, 6775.
- [44] The experimentally observed differences for these In–C bond lengths are 0.041(18) and –0.015(19) Å, respectively; neither of these is statistically significant.
- [45] Rahman, A. F. M. M.; Siddiqui, K. F.; Oliver, J. P. *Organometallics* **1982**, *1*, 881.
- [46] Downs, A. J.; Greene, T. M.; Parsons, S.; Taylor, R. A. Unpublished results.